THE JOURNAL OF PHYSICAL CHEMISTRY C

Article

Cite This: J. Phys. Chem. C 2018, 122, 17067−17072

pubs.acs.org/JPCC

Predicted Binary Compounds of Tin and Sulfur

Vu Ngoc Tuoc*,† and Tran Doan Huan*,‡,§,∥

†Institute of Engineering Physics, Hanoi University of Science and Technology, 1 Dai Co Viet Rd., Hanoi, Vietnam

‡Advanced Functional Materials for Energy and Environmental Applications Research Group, Ton Duc Thang University, Ho Chi Minh City, Vietnam

§Faculty of Applied Sciences, Ton Duc Thang University, Ho Chi Minh City, Vietnam

∥Institute of Materials Science, University of Connecticut, Storrs, Connecticut 06269, United States

Supporting Information

ABSTRACT: Three known binary compounds of tin (Sn) and sulfur (S), namely, SnS, SnS_2, and Sn_2S_3, have been extensively studied for potential application in energy generation and conversion applications. Inspired by the existence of many metastable phases of SnS, we explore the chemical space of nine crystalline solids with chemical composition Sn_xS_{1-x} (x falls between 0.25 and 0.75), predicting that Sn_3S is thermodynamically stable in a metallic $Pmn2_1$ phase. Due to the layered structure of this phase, Sn_3S is a quasi two-dimensional material, characterized by highly anisotropic electronic-related properties. Moreover, the discovered metastable structures of Sn_3S_2, Sn_2S, and Sn_5S_2 are just about 5 meV/atom above the stability limit, and may potentially be realized. The data set of 369 low-energy structures of nine Sn_xS_{1-x} crystalline solids reported in this work is a reliable sample of the low-energy sector of the chemical space, and thus being useful for the currently established materials databases, providing a playground for future data-mining works in materials discoveries.

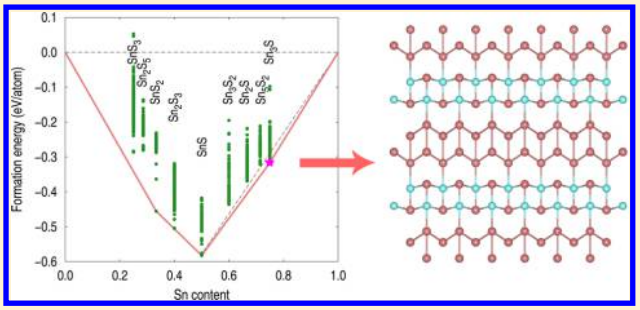

1. INTRODUCTION

Tin (Sn), a multivalent metal with several different oxidation states, is known to form three semiconducting solids with sulfur (S), including SnS, SnS_2, and Sn_2S_3.[1−15] The ground states of SnS and Sn_2S_3 both belong to the orthorhombic $Pnma$ (No. 62) space group,[1−4,6] while that of SnS_2 is a trigonal $P\bar{3}m1$ (No. 164) phase.[7,8] In different occasions, some other (metastable) phases of SnS, including an orthorhombic $Cmcm$,[16] the rocksalt,[17] and the zinc-blende,[18,19] have been realized. Very recently (in 2016), another metastable $P2_13$ (π-cubic) phase of SnS was experimentally discovered and resolved,[20,21] and then computationally studied.[22,23] This quite large (64 atoms per primitive cell) cubic structure is about 5−10 meV/atom higher than the $Pnma$ ground state, according to subsequent calculations.[14,20] Moreover,[24] a metallic phase of Sn_3S_4 was computationally predicted to be stable at pressures of about 15 GPa and above. It was not until the prediction/discoveries of the metastable phases were made that a great deal of interest has already been devoted to the potential applications of these materials, including photovoltaics,[1,5] thermoelectrics,[9−14] photodetector, and catalysis applications.[11,15]

The realization of many metastable phases of SnS (and other solid materials such as HfO_2[25] and $LiK(BH_4)_2$[26,27] as well) is inspirational. While these materials are attractive because of some novel functionalities they may offer,[23,25] their existence unambiguously indicates that materials discovery should really extend beyond the consideration of the ground states. In addition to the well-established experimental approaches, the recently developed theoretical/numerical methods are very effective in exploring such metastable materials, especially at extreme conditions, e.g., high temperature and pressure. Several notable examples of them include the first-principles based structure prediction methods[28] like USPEX[29,30] and minima-hopping[31,32] and a class of emerging data-mining approaches[33−35] developed recently following the strategic ideas and plans of the Materials Genome Initiative. These methods have led to plenty of successful applications, hence playing a central role in the future paradigm shift of materials discovery.[36−41]

The goal of this paper is two-fold. First, we aim at systematically exploring the demonstrated rich chemical space of the Sn_xS_{1-x} ($0.25 \le x \le 0.75$) binary compounds at ambient pressures. In particular, we searched for low-energy structures of 9 materials of this family, including SnS_3, Sn_2S_5, SnS_2, Sn_2S_3, SnS, Sn_3S_2, Sn_2S, Sn_5S_2, and Sn_3S, by the minima-hopping method. We then found that Sn_3S is thermodynamically stable with respect to the decomposition of other related materials and studied this new metallic material by calculations based on density functional theory (DFT).[42,43] Our prediction of Sn_3S

Received: May 7, 2018
Revised: July 2, 2018
Published: July 19, 2018

DOI: 10.1021/acs.jpcc.8b04328
J. Phys. Chem. C 2018, 122, 17067−17072

Table 1. Optimized Lattice Parameters *a*, *b*, and *c*, Given in Å, of the SnS (*Pnma* Phase), SnS_2 ($P\bar{3}m1$ Phase), and Sn_2S_3 (*Pnma* phase) with Five Numerical Flavors Considered[a]

material	phase		PBE	PBEsol	PBEsol + D3	vdW-DF2	DFT-D2	expt.
SnS	*Pnma*	*a*	4.02	3.99	3.96	4.13	4.01	3.98[6]
		b	4.43	4.21	4.18	4.72	4.27	4.33[6]
		c	11.42	11.10	11.01	12.08	11.39	11.18[6]
SnS_2	$P\bar{3}m1$	*a*	3.70	3.65	3.64	3.83	3.68	3.64[7]
		b	3.70	3.65	3.64	3.83	3.68	3.64[7]
		c	6.82	6.09	5.73	6.05	5.89	5.88[7]
Sn_2S_3	*Pnma*	*a*	3.80	3.76	3.76	3.93	3.78	3.77[4]
		b	9.27	8.79	8.63	9.47	8.87	8.88[4]
		c	14.43	13.79	13.64	14.54	13.98	14.02[4]

[a]The symmetry and, hence, the computed cell angles of the *Pnma* and $P\bar{3}m1$ phases are preserved. Relevant experimental data are provided with reference.

aligns well with the recent trend of materials discovery,[39,44] revealing that new binary materials with unusual stoichiometries, e.g., $NaCl_3$,[44] Na_3Au_2,[45] Li_3Al_2, Li_9Al_4, and $LiAl_3$,[46] and Mg_9Si_5,[39,47] can be found. Second, we provided the community a sizable and reliable data set of 369 new low-energy crystalline structures. Being prepared by an extensive structure search at the first-principles level, such a materials structure data set,[39,48,49] is an *adequate* sample of the low-energy sector of the chemical space. Given its relatively large size, it is able to comply with three over four V's (volume, variety, and veracity) of Big Data, and thus complementing the established materials databases, e.g., Materials Project,[50] Open Quantum Materials Database,[51] AFLOW,[52] and Polymer Genome,[53,11] the essential infrastructures of the emerging era of materials informatics.[33,40,54]

2. DETAILS OF THE METHODS

Our DFT calculations were performed with the Vienna *Ab initio* Simulation Package (VASP),[55−58] employing a plane-wave basis set with the kinetic energy up to 600 eV. The Brillouin zones were sampled by well-converged Monkhorst−Pack *k*-point meshes,[59] i.e., no less than 7 × 7 × 7. Convergence in optimizing the structures was assumed when the atomic forces become less than 0.01 eV/Å. The phonon frequency spectrum of the examined structure was computed within the supercell approach as implemented in the PHONOPY package.[60,61] The structure symmetry was analyzed using FINDSYM,[62,12] while VESTA[63,13] was used for visualization.

Because most of the known structures of SnS, SnS_2, and Sn_2S_3 are layered, van der Waals (vdW) interactions must be incorporated in the calculations.[10,12,24] In order to identify the best numerical scheme, we have optimized the ground state structures of SnS, SnS_2, and Sn_2S_3 using the (1) Perdew−Burke−Ernzerhof (PBE)[64] exchange-correlation (XC) energies functional, (2) PBEsol[65] XC functional, (3) PBESol + DFT-D3, (4) the nonlocal density functional vdW-DF2,[66] and (5) the DFT-D2 method of Grimme[67] to estimate the vdW interactions. The geometry of the optimized structures, given in Table 1, indicates that using DFT-D2 for the van der Waals interactions is the best numerical solution to recover the experimental data of SnS, SnS_2, and Sn_2S_3, and thus this prescription was used in our calculations. Some previous computational works[24] have also used this method for several Sn_xS_{1-x} solids.

The minima-hopping method was used to search for low-energy structures of the Sn_xS_{1-x} binary solids. In this method, the landscape of DFT energy (incorporating the DFT-D2 correction, according to the aforementioned examination) is explored by alternating molecular-dynamics runs for escaping the current local minimum and geometry optimization runs for identifying the next local minimum. Although the searches are relatively expensive, the predicted structures are reliable,[36−40,68] hereby soon leading to experimental confirmations.[25,41,69] In this work, the low-energy structures identified for a given chemical composition were assumed to be distinct if they are simultaneously different by (1) 5 meV/atom, (2) 3% in volume per atom, (3) 15% in average number of nearest S neighbors of Sn, and (4) 5% in averaged Sn−S bond length. For the last two criteria, i.e., (3) and (4), the Sn−S bond length cutoff is chosen to be 3.3 Å. All the criteria were chosen to be higher than the numerical errors of DFT computations, and the combination of the criteria can eliminate any further errors in the decision making. The data set and its details can be found in the Supporting Information.[70]

3. RESULTS AND DISCUSSION

3.1. Thermodynamic Stability. In order to access the thermodynamic stability of the identified structures, we computed the formation DFT energy ΔE_{DFT}, defined as

$$\Delta E_{DFT} = E_{DFT}(Sn_xS_{1-x}) - [xE_{DFT}(Sn) + (1 - x)E_{DFT}(S)] \quad (1)$$

Here, $E_{DFT}(Sn_xS_{1-x})$, $E_{DFT}(Sn)$, and $E_{DFT}(S)$ are the DFT energies computed for Sn_xS_{1-x}, the ground state cubic $Fd\bar{3}m$ structure of Sn, and orthorhombic *Fddd* structure of S.[71] The excellent agreement between the computed and measured formation energies for SnS, SnS_2, and Sn_2S_3, is shown in Table 2 as a validation of our computational scheme.

The convex hull constructed from ΔE_{DFT} computed for 369 predicted structures of 9 Sn_xS_{1-x} binary compounds is shown in Figure 1. Consistent with recent reports,[9,12] the ground states of SnS, SnS_2, and Sn_2S_3 are on a straight line, indicating that these materials can coexist and any of them can be

Table 2. Computed Formation Energy of SnS, SnS_2, and Sn_2S_3 Given with Respect to Relevant Experimental Data

		ΔE_{DFT}		
material	phase	(eV/atom)	(kJ/mol)	$\Delta E_{expt.}$ (kJ/mol)
SnS	*Pnma*	−0.580	−110	−100 to −108[72,73]
SnS_2	$P\bar{3}m1$	−0.460	−133	−148 to −182[73,74]
Sn_2S_3	*Pnma*	−0.505	−244	−249 to −297[73,74]

DOI: 10.1021/acs.jpcc.8b04328
J. Phys. Chem. C 2018, 122, 17067−17072

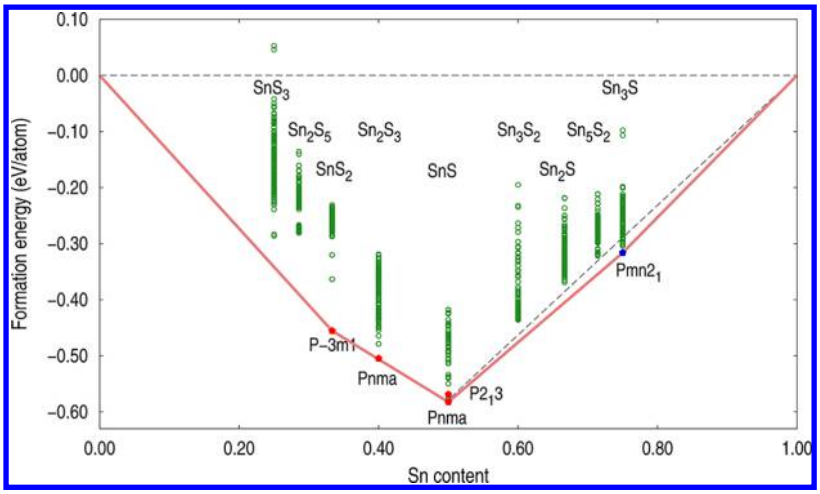

Figure 1. Convex hull (red solid line), constructed from the DFT formation energy of the 369 low-energy structures predicted for SnS_3, Sn_2S_5, SnS_2, Sn_2S_3, SnS, Sn_3S_2, Sn_2S, Sn_5S_2, and Sn_3S. Red pentagons mark some important experimentally realized phases of SnS_2, Sn_2S_3, and SnS, while the blue pentagon marks the predicted $Pmn2_1$ structure of Sn_3S. The dashed line connecting SnS and Sn is used to highlight the stability of Sn_3S.

transformed into the others without energy cost. Interestingly, Figure 1 also suggests that, in additional to these three known binaries of Sn and S, a new member of this family with the chemical composition Sn_3S is also thermodynamically stable. The lowest-energy structure of Sn_3S, which belongs to the $Pmn2_1$ space group, is about 25 meV/atom below the straight line connecting SnS and Sn, implying that the reaction SnS + 2Sn → Sn_3S is energetically favorable. Three other materials, including Sn_3S_2, Sn_2S, and Sn_5S_2 are above the convex hull (or the stability limit) by just about 5 meV/atom, an energy amount which is comparable with the vibrational free energy and the thermal energy (at 300 K, $k_BT \simeq 25$ meV). Specifically, Sn_5S_2 is equivalent with SnS and Sn in terms of stability; i.e., it can coexist with these two known solids. This observation suggests that there are good chances for at least Sn_3S, and maybe Sn_3S_2, Sn_2S, and Sn_5S_2, to be synthesized experimentally.

3.2. Sn_3Sn. The predicted orthorhombic $Pmn2_1$ structure of Sn_3S has three lattice parameters (optimized with DFT-D2) a = 3.982 Å, b = 12.950 Å, and c = 4.000 Å. Three Sn atoms and one S atom occupy the 2a Wyckoff positions (x = 0.000, y = −0.178, z = 0.129), (x = 0.000, y = 0.076, z = 0.129), (x = 0.000, y = 0.378, z = 0.145), and (x = 0.000, y = −0.418, z = 0.179), respectively. This structure, which is visualized in Figure 2, is composed of alternating topologically similar SnS and Sn layers; the former can be obtained from the latter just by replacing a Sn by a S atom. Moreover, these layers are very similar to that of the ground state *Pnma* structure of SnS (see Figure S1 and Table S2 of the Supporting Information[70] for a more detailed comparison). According to the computed phonon spectrum given in Figure S2 of the Supporting Information, the predicted structure of Sn_3S is dynamically stable.[70]

From the layered structural motif of Sn_3S, it could be predicted that the electronic properties of this Sn-rich materials are characterized by the those of the Sn and SnS layered constituents; the latter is likely semiconducting due to the aforementioned similarity with the semiconducting SnS. The computed electronic band structure of the $Pmn2_1$ phase of Sn_3S, which is shown in Figure 3a, indicates that this material is indeed metallic, the characteristics that can naturally be expected from the Sn layers of the structure. Indeed, the site-

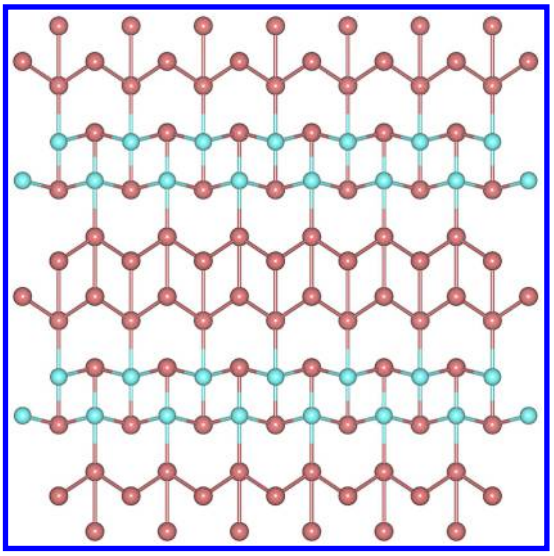

Figure 2. The $Pmn2_1$ phase of Sn_3S with a layered structural motif. Sn and S atoms are shown in blush and light cyan colors.

projected density of electronic states (DOS) shown in Figure 3b confirms that DOS near the Fermi level of Sn_3S is dominated by the Sn layers while contributions from the SnS layers are small. We have then performed a Bader charge analysis[75] of the $Pmn2_1$ structure of Sn_3S and the *Pnma* structure of SnS. The results (shown in the Supporting Information[70]) reveal that the charge transfer within the SnS layer of Sn_3S is essentially similar to that of SnS (about 2.1e from a Sn atom to a S atom), while the electronic coupling between the SnS and the Sn layers is weak; i.e., there is about 0.1e/Sn atom charge transfer between these layers.

This electronically decoupled nature of Sn_3S clearly hints that its electrical conductivity is anisotropic; e.g., the in-plane conductivity is high, whereas the out-of-plane conductivity is low. For a more quantitative assessment into this characteristics, we have used BoltzTraP[76] to estimate the electrical conductivity tensor σ of Sn_3S. This computational work involves computing the electronic bands of the $Pmn2_1$ structure on a very dense k-point grid (we used 39 × 12 × 39 here), from which the smooth interpolation of the bands

DOI: 10.1021/acs.jpcc.8b04328
J. Phys. Chem. C 2018, 122, 17067−17072

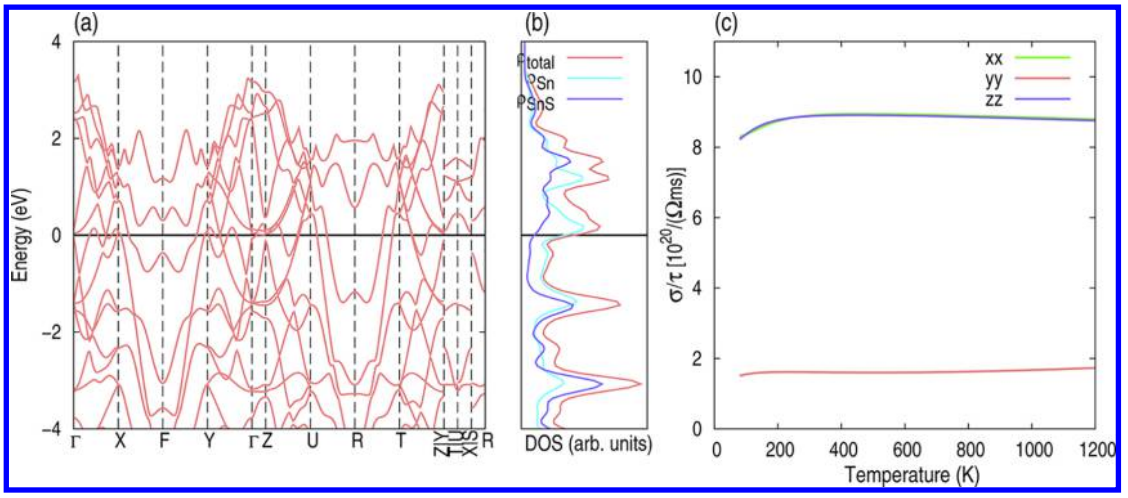

Figure 3. Electronic structure (a), electronic density of states (b), and the electrical conductivities (c, in unit of the relaxation time τ) of the $Pmn2_1$ phase of Sn_3S.

can be obtained, and hence the transport coefficients. Within this scheme, the relaxation time τ remains inaccessible, and thus σ/τ is the quantity that can actually be computed. The computed results of σ/τ are shown in Figure 3c, indicating that the in-plane (xx and zz) electrical conductivity is about 1 order higher than the out-of-plane (yy) conductivity. Therefore, from the electronic point of view, Sn_3S, supposed to be in its $Pmn2_1$ phase, can be considered an "effective" two-dimensional metallic material.

3.3. Implications and Perspectives. The $Pmn2_1$ phase of Sn_3S is predicted to be thermodynamically stable with respect to the decomposition into SnS and Sn, two well-known related solid materials. Although this is a very strong "green" signal, it still does not guarantee the existence of this hypothetical material because other factors, e.g., kinetic, also play important roles. Given that the constituent SnS layer of Sn_3S is just a slight deformation of that of the ground state *Pnma* structure of SnS, Sn_3S may be formed in a mixture of SnS and Sn under some conditions that may facilitate the reaction of these solids. For some other metastable materials, i.e., Sn_3S_2, Sn_2S, and Sn_5S_2, which are about 5 meV/atom above the convex hull (Figure 1), there are still chances for them to be synthesized just like the metastable phases of SnS discussion in section 1. From the computational point of view, the recently introduced "amorphous limit",[77] which can be computed, can give some insights into the synthesizability of these metastable structures. A more detailed analysis based on this concept is out of the scope of this work and may be the goal of future studies.

The abundance of the chemical space of Sn_xS_{1-x} materials is clearly evident. While our discussion here is limited within the thermodynamic consideration based on computations at zero temperature only, it will not be a surprise if external conditions like pressure and temperature can stabilize some of the metastable structures, for which some new properties may then be found. The prediction of Sn_3S clearly indicates that studying the family of Sn_xS_{1-x} solid materials remains an open avenue of materials discovery.

On the other hand, the data set reported here for the low-energy structures of Sn_xS_{1-x} solids is valuable for the community. The key value of this data set is that, because it was prepared by systematic first-principles based structure searches, it is significantly diverse, adequately sampling the low-energy sector of the chemical space. As statistical learning is joining the main stream of materials science, insightful information can be obtained by appropriately mining well-curate big data sets.[40,77] This is the motivation behind the development of Materials Project,[50] Open Quantum Materials Database,[51] AFLOW,[52] and Polymer Genome,[53] which aim to provide essential resource for the future approaches of materials discovery. Within this context, materials structure data sets prepared from structure prediction works[39,48,49] can effectively contribute to the development of the materials databases. As an example, a similar data set of more than 300 Mg/Si binary compounds has recently been available in Materials Project, significantly diversifying the Mg/Si subset of this well-known database.[39]

4. CONCLUSIONS

By exploring the chemical space of nine Sn_xS_{1-x} crystalline solids with x falls between 0.25 and 0.75, we predict that Sn_3S is thermodynamically stable in a metallic $Pmn2_1$ phase. Because of the layered structure, the electronic properties of this material are decoupled into contributions from the atomic-thin metallic Sn and the semiconducting SnS layers, and thus, its electrical conductivity is highly anisotropic. Some other solids, i.e., Sn_3S_2, Sn_2S, and Sn_5S_2, are just about 5 meV/atom above the convex hull and there may be chances for them to be synthesized. The data set of 369 low-energy structures of 9 Sn_xS_{1-x} crystalline solids provided in this work is useful for the established materials databases and future data-mining based works in materials discoveries.

■ ASSOCIATED CONTENT

Supporting Information

The Supporting Information is available free of charge on the ACS Publications website at DOI: 10.1021/acs.jpcc.8b04328.

Data files in .cif format (ZIP)

(1) The content of the data set of 9 Sn_xS_{1-x} crystalline solids, (2) detailed comparison between Sn_3S and SnS, and (3) the computed phonon band structure of the $Pmn2_1$ phase of Sn_3S (PDF)

■ AUTHOR INFORMATION

Corresponding Authors

*E-mail: tuoc.vungoc@hust.edu.vn (V.N.T.).

DOI: 10.1021/acs.jpcc.8b04328
J. Phys. Chem. C 2018, 122, 17067−17072

*E-mail: trandoanhuan@tdt.edu.vn (T.D.H.).

ORCID

Vu Ngoc Tuoc: 0000-0002-5749-1483

Tran Doan Huan: 0000-0002-8093-9426

Notes

The authors declare no competing financial interest.

■ ACKNOWLEDGMENTS

V.N.T. and T.D.H. equally contributed to this work. T.D.H. acknowledges computational support from XSEDE under the grant number TG-DMR170031. Work by V.N.T. is supported by the Vietnamese National Foundation for Science and Technology Development (NAFOSTED) under Grant number 103.01-2017.24.

■ REFERENCES

(1) Ramakrishna Reddy, K. T.; Koteswara Reddy, N.; Miles, R. Photovoltaic properties of SnS based solar cells. *Sol. Energy Mater. Sol. Cells* **2006**, *90*, 3041−3046.

(2) Zainal, Z.; Hussein, M. Z.; Ghazali, A. Cathodic electrodeposition of SnS thin films from aqueous solution. *Sol. Energy Mater. Sol. Cells* **1996**, *40*, 347−357.

(3) Baek, I.-H.; Pyeon, J. J.; Song, Y. G.; Chung, T.-M.; Kim, H.-R.; Baek, S.-H.; Kim, J.-S.; Kang, C.-Y.; Choi, J.-W.; Hwang, C. S.; et al. Synthesis of SnS Thin Films by Atomic Layer Deposition at Low Temperatures. *Chem. Mater.* **2017**, *29*, 8100−8110.

(4) Kniep, R.; Mootz, D.; Severin, U.; Wunderlich, H. Structure of tin(II) tin(IV) trisulphide, a redetermination. *Acta Crystallogr., Sect. B: Struct. Crystallogr. Cryst. Chem.* **1982**, *38*, 2022−2023.

(5) Patel, M.; Kim, H.-S.; Kim, J. Wafer-scale production of vertical SnS multilayers for high-performing photoelectric devices. *Nanoscale* **2017**, *9*, 15804−15812.

(6) Hofmann, W. Ergebnisse der strukturbestimmung komplexer sulfide. *Z. Kristallogr. - Cryst. Mater.* **1935**, *92*, 161−185.

(7) Hazen, R. M.; Finger, L. W. The crystal structures and compressibilities of layer minerals at high pressure; I, SnS < 2), berndtite. *Am. Mineral.* **1978**, *63*, 289−292.

(8) Su, G.; Hadjiev, V. G.; Loya, P. E.; Zhang, J.; Lei, S.; Maharjan, S.; Dong, P.; Ajayan, P. M.; Lou, J.; Peng, H. Chemical Vapor Deposition of Thin Crystals of Layered Semiconductor SnS_2 for Fast Photodetection Application. *Nano Lett.* **2015**, *15*, 506−513.

(9) Burton, L. A.; Walsh, A. Phase Stability of the Earth-Abundant Tin Sulfides SnS, SnS_2, and Sn_2S_3. *J. Phys. Chem. C* **2012**, *116*, 24262−24267.

(10) Whittles, T. J.; Burton, L. A.; Skelton, J. M.; Walsh, A.; Veal, T. D.; Dhanak, V. R. Band Alignments, Valence Bands, and Core Levels in the Tin Sulfides SnS, SnS_2, and Sn_2S_3: Experiment and Theory. *Chem. Mater.* **2016**, *28*, 3718−3726.

(11) Skelton, J. M.; Burton, L. A.; Jackson, A. J.; Oba, F.; Parker, S. C.; Walsh, A. Lattice dynamics of the tin sulphides SnS_4, SnS and Sn_2S_3: vibrational spectra and thermal transport. *Phys. Chem. Chem. Phys.* **2017**, *19*, 12452−12465.

(12) Skelton, J. M.; Burton, L. A.; Oba, F.; Walsh, A. Chemical and Lattice Stability of the Tin Sulfides. *J. Phys. Chem. C* **2017**, *121*, 6446−6454.

(13) Guo, R.; Wang, X.; Kuang, Y.; Huang, B. First-principles study of anisotropic thermoelectric transport properties of IV-VI semiconductor compounds SnSe and SnS. *Phys. Rev. B: Condens. Matter Mater. Phys.* **2015**, *92*, 115202.

(14) Segev, E.; Argaman, U.; Abutbul, R. E.; Golan, Y.; Makov, G. A new cubic prototype structure in the IV-VI monochalcogenide system: a DFT study. *CrystEngComm* **2017**, *19*, 1751−1761.

(15) Kilner, J. A., Skinner, S. J., Irvine, S. J. C., Edwards, P. P., Eds. *Functional Materials for Sustainable Energy Applications*; Woodhead Publishing: Cambridge, U.K., 2012.

(16) von Schnering, H. G.; Wiedemeier, H. The high-temperature structure of beta-Sns and beta-SnSe and the B16-to-B33 type Lambda-transition path. *Z. Kristallogr. - Cryst. Mater.* **1981**, *156*, 143−150.

(17) Mariano, A. N.; Chopra, K. L. Polymorphism in Some Iv-Vi Compounds Induced by High Pressure and Thin-Film Epitaxial Growth. *Appl. Phys. Lett.* **1967**, *10*, 282−284.

(18) Greyson, E. C.; Barton, J. E.; Odom, T. W. Tetrahedral zinc blende tin sulfide nano- and microcrystals. *Small* **2006**, *2*, 368−371.

(19) Avellaneda, D.; Nair, M. T. S.; Nair, P. K. Polymorphic tin sulfide thin films of zinc blende and orthorhombic structures by chemical deposition. *J. Electrochem. Soc.* **2008**, *155*, D517−D525.

(20) Abutbul, R. E.; Segev, E.; Zeiri, L.; Ezersky, V.; Makov, G.; Golan, Y. Synthesis and properties of nanocrystalline π-SnS - a new cubic phase of tin sulphide. *RSC Adv.* **2016**, *6*, 5848−5855.

(21) Abutbul, R. E.; Garcia-Angelmo, A. R.; Burshtein, Z.; Nair, M. T. S.; Nair, P. K.; Golan, Y. Crystal structure of a large cubic tin monosulfide polymorph: an unraveled puzzle. *CrystEngComm* **2016**, *18*, 5188−5194.

(22) Mahdi, M. S.; Ibrahim, K.; Hmood, A.; Ahmed, N. M.; Mustafa, F. I.; Azzez, S. A. High performance near infrared photodetector based on cubic crystal structure SnS thin film on a glass substrate. *Mater. Lett.* **2017**, *200*, 10−13.

(23) Skelton, J. M.; Burton, L. A.; Oba, F.; Walsh, A. Metastable cubic tin sulfide: A novel phonon-stable chiral semiconductor. *APL Mater.* **2017**, *5*, 036101.

(24) Gonzalez, J. M.; Kien, N. C.; Steele, B. A.; Oleynik, I. I. Ambient and high pressure phases of tin sulfide compounds. **2017**, arXiv:1710.03642 [cond-mat.mtrl-sci], arXiv.org e-Print archive.

(25) Huan, T. D.; Sharma, V.; Rossetti, G. A.; Ramprasad, R. Pathways towards ferroelectricity in hafnia. *Phys. Rev. B: Condens. Matter Mater. Phys.* **2014**, *90*, 064111.

(26) Tuan, L.; Nguyen, C. K.; Huan, T. D. First-principles prediction for the stability of $LiK(BH_4)_2$. *Phys. Status Solidi B* **2014**, *251*, 1539−1544.

(27) Ley, M. B.; Roedern, E.; Jensen, T. R. Eutectic melting of $LiBH_4$-KBH_4. *Phys. Chem. Chem. Phys.* **2014**, *16*, 24194−24199.

(28) Oganov, A. R., Ed. *Modern Methods of Crystal Structure Prediction*; Wiley-VCH: Weinheim, Germany, 2011.

(29) Glass, C. W.; Oganov, A. R.; Hansen, N. USPEX-Evolutionary crystal structure prediction. *Comput. Phys. Commun.* **2006**, *175*, 713−720.

(30) Oganov, A. R.; Glass, C. W. Crystal structure prediction using ab initio evolutionary techniques: Principles and applications. *J. Chem. Phys.* **2006**, *124*, 244704.

(31) Goedecker, S. Minima hopping: An efficient search method for the global minimum of the potential energy surface of complex molecular systems. *J. Chem. Phys.* **2004**, *120*, 9911.

(32) Amsler, M.; Goedecker, S. Crystal structure prediction using the minima hopping method. *J. Chem. Phys.* **2010**, *133*, 224104.

(33) Rajan, K. Materials informatics. *Mater. Today* **2005**, *8*, 38−45.

(34) Jain, A.; Shin, Y.; Persson, K. A. Computational predictions of energy materials using density functional theory. *Nat. Rev. Mater.* **2016**, *1*, 15004.

(35) Xiang, H. J.; Huang, B.; Kan, E.; Wei, S.-H.; Gong, X. G. Towards Direct-Gap Silicon Phases by the Inverse Band Structure Design Approach. *Phys. Rev. Lett.* **2013**, *110*, 118702.

(36) Huan, T. D.; Amsler, M.; Tuoc, V. N.; Willand, A.; Goedecker, S. Low-energy structures of zinc borohydride $Zn(BH_4)_2$. *Phys. Rev. B: Condens. Matter Mater. Phys.* **2012**, *86*, 224110.

(37) Huan, T. D.; Amsler, M.; Sabatini, R.; Tuoc, V. N.; Le, N. B.; Woods, L. M.; Marzari, N.; Goedecker, S. Thermodynamic stability of alkali metal/zinc double-cation borohydrides at low temperatures. *Phys. Rev. B: Condens. Matter Mater. Phys.* **2013**, *88*, 024108.

(38) Huan, T. D.; Tuoc, V. N.; Minh, N. V. Layered structures of organic/inorganic hybrid halide perovskites. *Phys. Rev. B: Condens. Matter Mater. Phys.* **2016**, *93*, 094105.

(39) Huan, T. D. Pressure-stabilized binary compounds of magnesium and silicon. *Phys. Rev. Materials* **2018**, *2*, 023803. The materials data set reported in the following paper is available in

Materials Project (https://materialsproject.org/) and can also be accessed via https://doi.org/10.17188/1432992.
(40) Huan, T. D.; Mannodi-Kanakkithodi, A.; Ramprasad, R. Accelerated materials property predictions and design using motif-based fingerprints. *Phys. Rev. B: Condens. Matter Mater. Phys.* **2015**, *92*, 014106.
(41) Tran, H. D.; Amsler, M.; Botti, S.; Marques, M. A. L.; Goedecker, S. First-principles predicted low-energy structures of $NaSc(BH_4)_4$. *J. Chem. Phys.* **2014**, *140*, 124708.
(42) Hohenberg, P.; Kohn, W. Inhomogeneous electron gas. *Phys. Rev.* **1964**, *136*, B864−B871.
(43) Kohn, W.; Sham, L. Self-consistent equations including exchange and correlation effects. *Phys. Rev.* **1965**, *140*, A1133−A1138.
(44) Zhang, W.; Oganov, A. R.; Goncharov, A. F.; Zhu, Q.; Boulfelfel, S. E.; Lyakhov, A. O.; Stavrou, E.; Somayazulu, M.; Prakapenka, V. B.; Konôpková, Z. Unexpected stable stoichiometries of sodium chlorides. *Science* **2013**, *342*, 1502−1505.
(45) Sarmiento-Pérez, R.; Cerqueira, T. F.; Valencia-Jaime, I.; Amsler, M.; Goedecker, S.; Botti, S.; Marques, M. A.; Romero, A. H. Sodium-gold binaries: novel structures for ionic compounds from an ab initio structural search. *New J. Phys.* **2013**, *15*, 115007.
(46) Sarmiento-Pérez, R.; Cerqueira, T. F. T.; Valencia-Jaime, I.; Amsler, M.; Goedecker, S.; Romero, A. H.; Botti, S.; Marques, M. A. L. Novel phases of lithium-aluminum binaries from first-principles structural search. *J. Chem. Phys.* **2015**, *142*, 024710.
(47) Jacobs, M. H. The structure of the metastable precipitates formed during ageing of an Al-Mg-Si alloy. *Philos. Mag.* **1972**, *26*, 1−13.
(48) Huan, T. D.; Mannodi-Kanakkithodi, A.; Kim, C.; Sharma, V.; Pilania, G.; Ramprasad, R. A polymer dataset for accelerated property prediction and design. *Sci. Data* **2016**, *3*, 160012.
(49) Kim, C.; Huan, T. D.; Krishnan, S.; Ramprasad, R. A hybrid organic-inorganic perovskite dataset. *Sci. Data* **2017**, *4*, 170057.
(50) Jain, A.; Ong, S. P.; Hautier, G.; Chen, W.; Richards, W. D.; Dacek, S.; Cholia, S.; Gunter, D.; Skinner, D.; Ceder, G.; et al. Commentary: The Materials Project: A materials genome approach to accelerating materials innovation. *APL Mater.* **2013**, *1*, 011002.
(51) Saal, J. E.; Kirklin, S.; Aykol, M.; Meredig, B.; Wolverton, C. Materials design and discovery with high-throughput density functional theory: the open quantum materials database (OQMD). *JOM* **2013**, *65*, 1501−1509.
(52) Taylor, R. H.; Rose, F.; Toher, C.; Levy, O.; Yang, K.; Nardelli, M. B.; Curtarolo, S. A RESTful API for exchanging materials data in the AFLOWLIB.org consortium. *Comput. Mater. Sci.* **2014**, *93*, 178−192.
(53) Mannodi-Kanakkithodi, A.; Chandrasekaran, A.; Kim, C.; Huan, T. D.; Pilania, G.; Botu, V.; Ramprasad, R. Scoping the polymer genome: A roadmap for rational polymer dielectrics design and beyond. *Mater. Today* **2017**, in press. DOI: 10.1016/j.mattod.2017.11.021.
(54) Hautier, G.; Jain, A.; Ong, S. From the computer to the laboratory: materials discovery and design using first-principles calculations. *J. Mater. Sci.* **2012**, *47*, 7317.
(55) Kresse, G.; Hafner, J. Ab initio molecular dynamics for liquid metals. *Phys. Rev. B: Condens. Matter Mater. Phys.* **1993**, *47*, 558−561.
(56) Kresse, G. Ab initio Molekular Dynamik für flüssige Metalle. Ph.D. Thesis, Technische Universität Wien, Wien, Austria, 1993.
(57) Kresse, G.; Furthmüller, J. Efficiency of ab-initio total energy calculations for metals and semiconductors using a plane-wave basis set. *Comput. Mater. Sci.* **1996**, *6*, 15−50.
(58) Kresse, G.; Furthmüller, J. Efficient iterative schemes for ab initio total-energy calculations using a plane-wave basis set. *Phys. Rev. B: Condens. Matter Mater. Phys.* **1996**, *54*, 11169−11186.
(59) Monkhorst, H. J.; Pack, J. D. Special points for Brillouin-zone integrations. *Phys. Rev. B* **1976**, *13*, 5188.
(60) Togo, A.; Oba, F.; Tanaka, I. First-principles calculations of the ferroelastic transition between rutile-type and $CaCl_2$-type SiO_2 at high pressures. *Phys. Rev. B: Condens. Matter Mater. Phys.* **2008**, *78*, 134106.
(61) Parlinski, K.; Li, Z. Q.; Kawazoe, Y. First-Principles Determination of the Soft Mode in Cubic ZrO_2. *Phys. Rev. Lett.* **1997**, *78*, 4063.
(62) FINDSYM. http://stokes.byu.edu/findsym.html.
(63) Momma, K.; Izumi, F. VESTA: a three-dimensional visualization system for electronic and structural analysis. *J. Appl. Crystallogr.* **2008**, *41*, 653.
(64) Perdew, J. P.; Burke, K.; Ernzerhof, M. Generalized Gradient Approximation Made Simple. *Phys. Rev. Lett.* **1996**, *77*, 3865−3868.
(65) Perdew, J. P.; Ruzsinszky, A.; Csonka, G. I.; Vydrov, O. A.; Scuseria, G. E.; Constantin, L. A.; Zhou, X.; Burke, K. Restoring the Density-Gradient Expansion for Exchange in Solids and Surfaces. *Phys. Rev. Lett.* **2008**, *100*, 136406.
(66) Lee, K.; Murray, É. D.; Kong, L.; Lundqvist, B. I.; Langreth, D. C. Higher-accuracy van der Waals density functional. *Phys. Rev. B: Condens. Matter Mater. Phys.* **2010**, *82*, 081101.
(67) Grimme, S. Semiempirical GGA-type density functional constructed with a long-range dispersion correction. *J. Comput. Chem.* **2006**, *27*, 1787.
(68) Huan, T. D.; Tuoc, V. N.; Le, N. B.; Minh, N. V.; Woods, L. M. High-pressure phases of Mg_2Si from first principles. *Phys. Rev. B: Condens. Matter Mater. Phys.* **2016**, *93*, 094109.
(69) Huan, T. D.; Amsler, M.; Marques, M. A. L.; Botti, S.; Willand, A.; Goedecker, S. Low-energy polymeric phases of alanates. *Phys. Rev. Lett.* **2013**, *110*, 135502.
(70) See the Supporting Information for more information reported in this paper.
(71) Warren, B. E.; Burwell, J. T. The structure of rhombic sulphur. *J. Chem. Phys.* **1935**, *3*, 6−8.
(72) Haynes, W. M., Ed. *CRC Handbook of Chemistry and Physics*; CRC Press: Boca Raton, FL, 2012.
(73) Sharma, R.; Chang, Y. The S-Sn (Sulfur-Tin) system. *Bull. Alloy Phase Diagrams* **1986**, *7*, 269−273.
(74) Novoselova, A.; Zlomanov, V.; Karbanov, S.; Matveyev, O.; Gas'kov, A. Physico-chemical study of the germanium, tin, lead chalcogenides. *Prog. Solid State Chem.* **1972**, *7*, 85−115.
(75) Tang, W.; Sanville, E.; Henkelman, G. A grid-based Bader analysis algorithm without lattice bias. *J. Phys.: Condens. Matter* **2009**, *21*, 084204.
(76) Madsen, G. K.; Singh, D. J. BoltzTraP. A code for calculating band-structure dependent quantities. *Comput. Phys. Commun.* **2006**, *175*, 67−71.
(77) Aykol, M.; Dwaraknath, S. S.; Sun, W.; Persson, K. A. Thermodynamic limit for synthesis of metastable inorganic materials. *Sci. Adv.* **2018**, *4*, eaaq0148.

DOI: 10.1021/acs.jpcc.8b04328
J. Phys. Chem. C 2018, 122, 17067−17072